Supporting Information of

Au-decorated hollow CuO with modulated electronic structure for efficient electrocatalytic glucose oxidation

Yan Yang,[a] Hao Chen,[a] Jiahui Ding,[a] Yonghui Shao,[a] Yanjie Fu,[a] Yunrui Huang,[a] Xiaodi Liu,[a,*] Bicheng Zhu,[b,c] Jadranka Travas-Sejdic[b,c,*]

[a]College of Chemical and Pharmaceutical Engineering, Nanyang Normal University, Nanyang, Henan, China

[b]Centre for Innovative Materials for Health, School of Chemical Sciences, University of Auckland-Waipapa Auckland, New Zealand

[c]MacDiarmid Institute for Advanced Materials and Nanotechnology, Wellington, New Zealand

E-mail address: liuxiaodiny@126.com (X. Liu); j.travas-sejdic@auckland.ac.nz(J. Travas-Sejdic)

Experimental details

Structural characterizations and electrochemical measurements: The crystal structures of the samples are researched on an X-ray diffractometer (XRD, Rigaku D/max-2500). An electron spectrometer (Thermo ESCALAB 250XI) is employed to analyze the X-ray photoelectron spectra (XPS) of the products. The Brunauer-Emmett-Teller (BET) specific surface areas of the products are determined using a Micromeritics Autosorb-iQ apparatus. The size, shape, composition, and nanostructure of the obtained samples are examined by transmission electron microscopy (TEM, JEM-2100), high-resolution TEM (HRTEM, JEM-2100), scanning electron microscopy (SEM, JSM 6700F), and energy dispersive X-ray spectroscopy (EDX).

Fabrication of electrodes: Firstly, a glassy carbon electrode (GCE, 3 mm diameter) is washed by ultrasonication in ultra-pure water for 5 min. Then, GCE is polished using 0.5 μm and 50 nm Al slurries and ultrasonically washed with ultra-pure water. Additionally, 5 mg of Au/N-CuO-HM is dispersed in 1 mL of ultra-pure water and ultrasonicated for 1 h to acquire a stable suspension. Subsequently, 10 μL of the suspension is deposited on GCE and dried under ambient condition to form Au/N-CuO-HM/GCE. Afterward, 5 μL of 0.05% Nafion (Nf) solution is dropped on the surface of Au/N-CuO-HM/GCE. Finally, the electrode is dried at room temperature to acquire the Au/N-CuO-HM modified electrode (Nf/Au/N-CuO-HM/GCE). For comparison, an N-CuO-HM-based electrode (Nf/N-CuO-HM/GCE) is prepared by replicating the above procedure.

Electrochemical measurements: Cyclic voltammetry (CV) and amperometric tests are carried out using a CHI 660E Electrochemical Workstation (Chenhua, China) equipped with a standard three-electrode system. The working electrodes consist of the as-obtained electrodes (bare GCE, Nf/Au/N-CuO-HM/GCE, or Nf/N-CuO-HM/GCE), with saturated calomel electrode (SCE) and Pt wire acting as reference electrode and counter electrode, respectively. Glucose detection is performed in 0.1 M NaOH aqueous solution at room temperature. CV measurements are recorded in a static solution. To ensure adequate mass transport, the amperometric current-time (*i*-*t*) curves are carried out under continuous magnetic stirring (200 rpm). The impedance behaviors of the as-obtained electrodes are researched using electrochemical impedance spectroscopy (EIS) in 0.1 M KCl solution containing 5 mM $[Fe(CN)_6]^{4-/3-}$.

Density functional theory (DFT) calculations: DFT calculations are performed using the

Vienna *Ab initio* Simulation Package (VASP) within the generalized gradient approximation (GGA) using the Perdew-Burke-Ernzerhof (PBE) functional. The projected augmented wave (PAW) method is employed to describe the ionic cores and take valence electrons, with a plane-wave cutoff energy of 450 eV. For geometry optimization, the Brillouin zone is performed using a Γ-centered 2×2×1 *k*-point mesh. Partial occupancies of the Kohn-Sham orbitals are allowed using the Gaussian smearing method and a width of 0.05 eV. Electronic self-consistency is considered as the energy difference fell below 10^{-5} eV. To account for the strong electron correlation effects in the transition metal, spin-polarized GGA+U with the Hubbard correction method is conducted, and the effective U_{eff} parameter is set to 4.0 eV for Cu. The CuO(111) surface is selected to build the CuO model due to its high thermodynamic stability and is constructed based on monoclinic CuO (space group C2/c) with lattice parameters of a = 4.653 Å, b = 3.41 Å, c = 5.108 Å, $\alpha = \gamma = 90°$, $\beta = 99.48°$. A vacuum layer of 18 Å is introduced along the *z*-axis perpendicular to the surface. The Au_{13} cluster is a feasible model for simulating Au catalysts in the theoretical analysis of glucose oxidation. Therefore, two slab models are constructed, including a clean CuO(111) surface and a CuO(111) surface supported with an Au_{13} cluster, denoted as CuO(111) and Au-CuO(111), respectively. Charge density difference, Bader charge analysis, total density of states (TDOS), and projected density of states (PDOS) are calculated to probe charge redistribution and electronic structure. In addition, the adsorption energy (E_{ads}) of glucose on the substrate is calculated by $E_{ads} = E_{total} - (E_{slab} + E_{glu})$, in which E_{total}, E_{slab}, and E_{glu} represent the total energy of the substrate with adsorbed glucose, the energy of the CuO(111) or Au13-CuO(111), and the energy of the adsorbed glucose molecule, respectively.

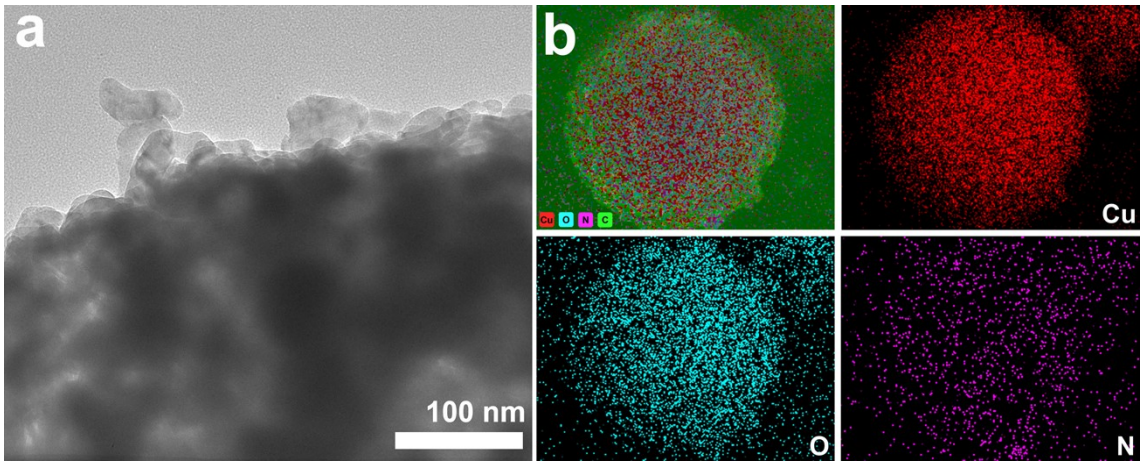

Fig. S1 (a) High-magnification TEM image of Au/N-CuO-HM; (b) EDX elemental mapping images of N-CuO-HM.

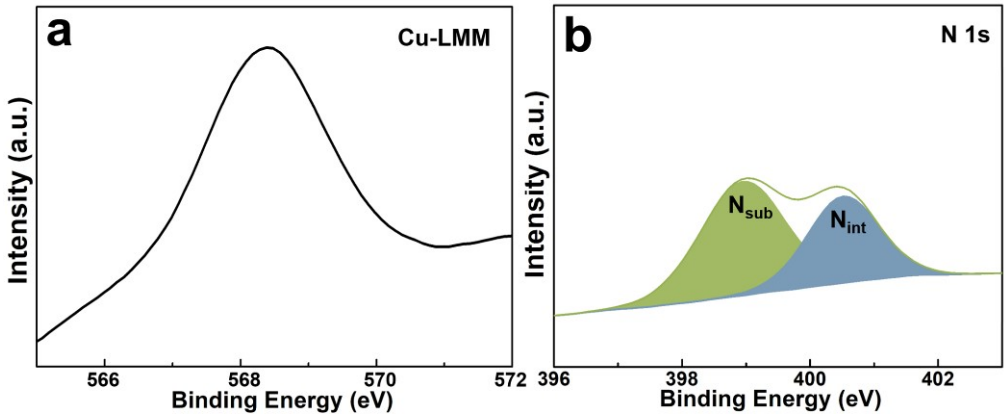

Fig. S2 (a) Cu LMM Auger spectrum and (b) N 1s XPS spectrum of Au/N-CuO-HM.

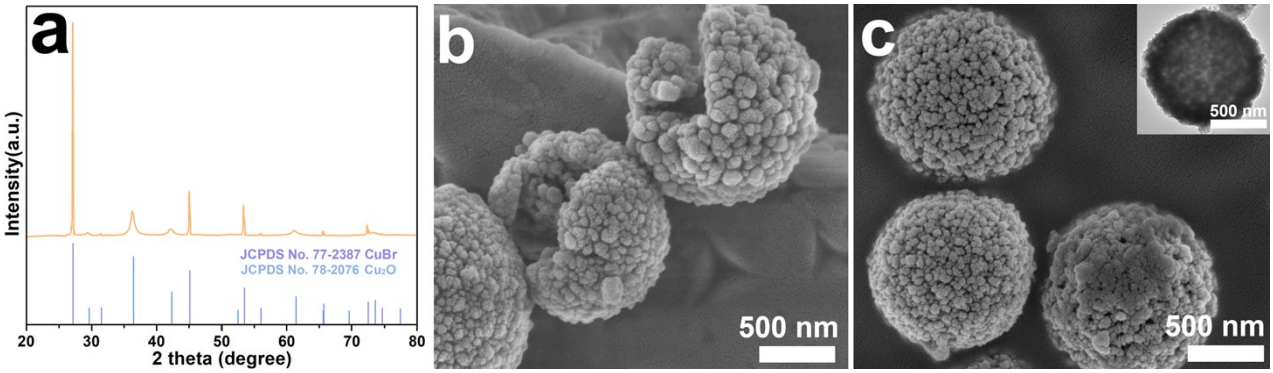

Fig. S3 (a) XRD pattern of the CuBr/Cu_2O precursor; (b) SEM image the CuBr/Cu_2O precursor synthesized at 6 h; (c) SEM and TEM images of the CuBr/Cu_2O precursor synthesized at 12 h.

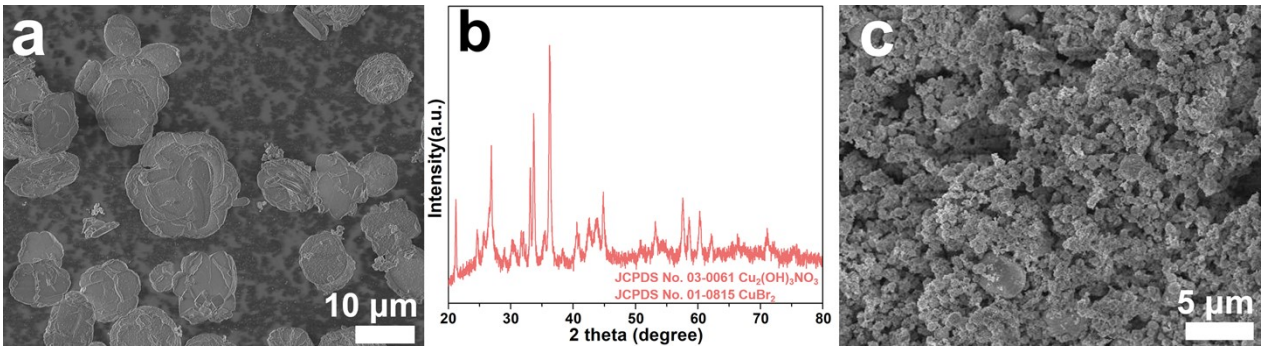

Fig. S4 (a) SEM image and (b) XRD pattern of the products synthesized under the same conditions as the CuBr/Cu_2O precursor but without glycerol (18 mL ethanol as the sole solvent); (c) SEM image of CuO-NP synthesized under the same conditions as N-CuO-HM but without [C_{16}mim]Br.

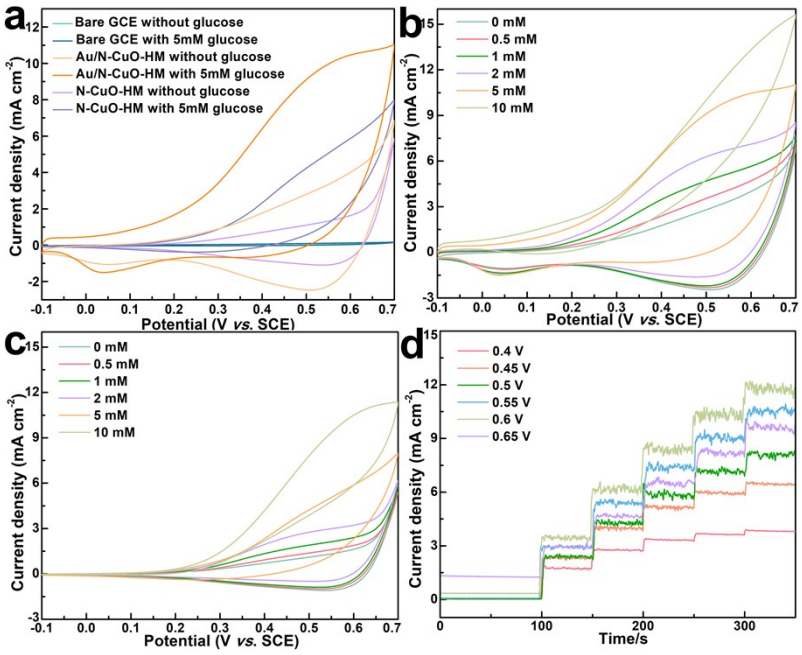

Fig. S5 (a) CV curves of differentt electrodes in 0.1 M NaOH with and without 5 mM glucose; CV curves of (b) Nf/Au/N-CuO-HM/GCE and (c) Nf/N-CuO-HM/GCE with different glucose concentrations; (d) Amperometric responses of Nf/Au/N-CuO-HM/GCE at various working potential.

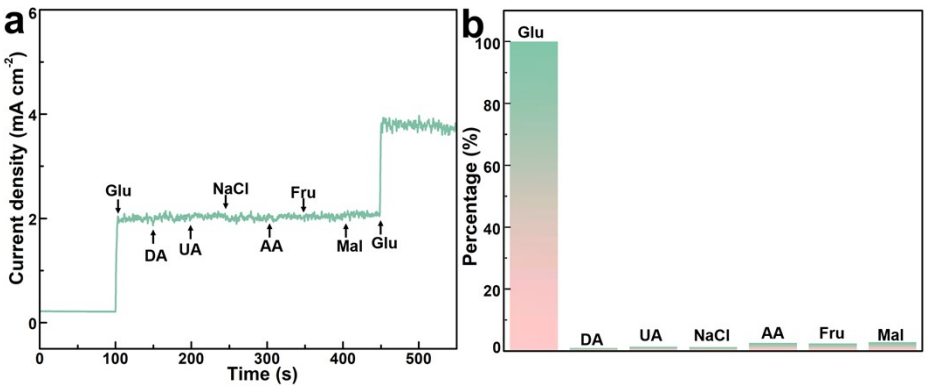

Fig. S6 (a) Amperometric response profiles of Nf/Au/N-CuO-HM/GCE upon the successive addition of glucose and various interfering species in 0.1 M NaOH solution; (b) Percentage contribution of the interfering signals compared to the glucose signal.

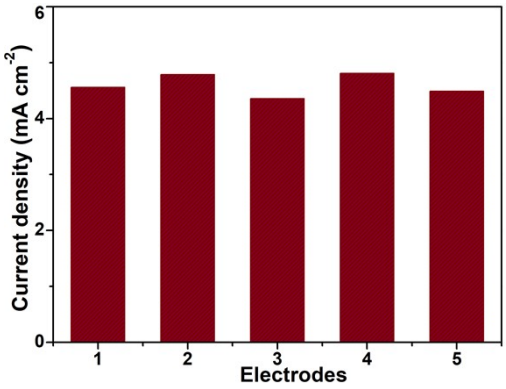

Fig. S7 Comparison of the current densities of five different electrodes in 0.1 M NaOH solution with the addition of 0.5 mM glucose.

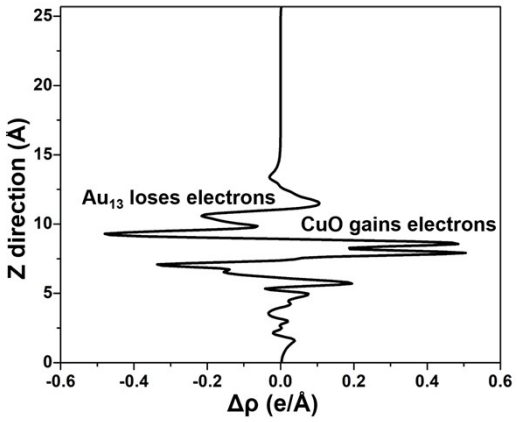

Fig. S8 Line profile of the charge density difference along the *z*-axis for the Au/CuO interface.

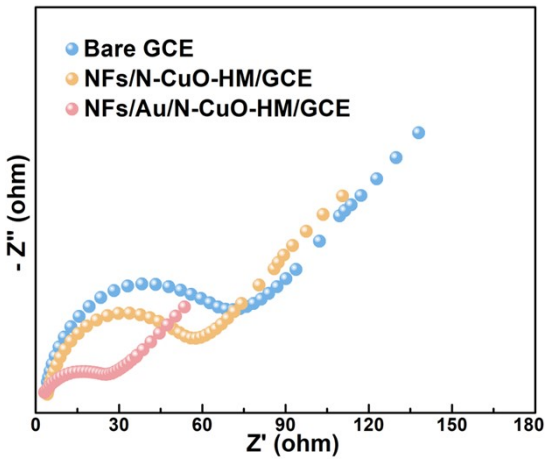

Fig. S9 Nyquist plots of bare GCE, Nf/N-CuO-HM/GCE, and Nf/Au/N-CuO-HM/GCE in 0.1 M KCl solution containing 5 mM $[Fe(CN)_6]^{3-/4-}$.

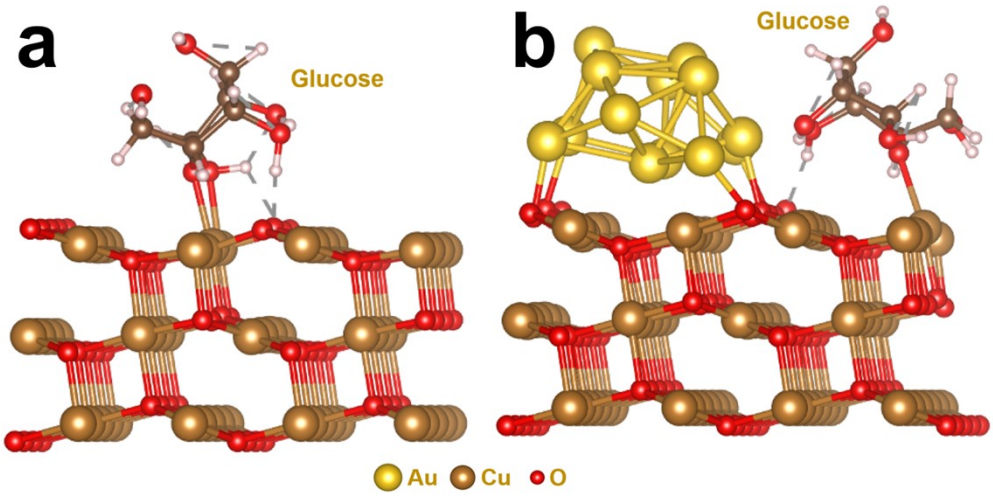

Fig. S10 Optimized adsorption structures of glucose on (a) Cu(111) and (b) Au-CuO(111).

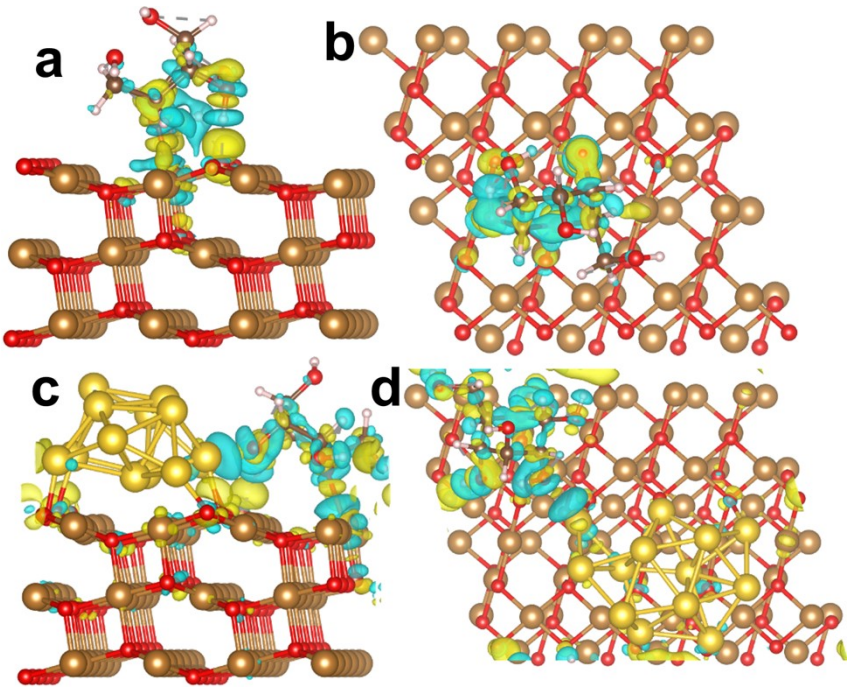

Fig. S11 (a) Side-view and (b) top-view of charge density difference between glucose and CuO(111); (c) Side-view and (d) top-view of charge density difference between glucose and Au-CuO(111).

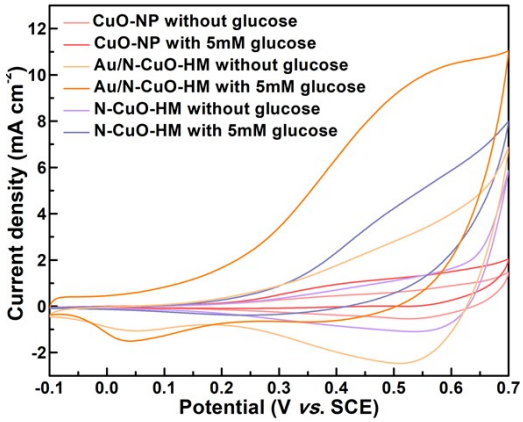

Fig. S12 CV curves of Nf/CuO-NP/GCE, Nf/N-CuO-HM/GCE, and Nf/Au/N-CuO-HM/GCE in 0.1 M NaOH with and without 5 mM glucose.